

Highly Selective Syngas/H₂ Production via Partial Oxidation of CH₄ Using (Ni, Co and Ni/Co)/ZrO₂/Al₂O₃ Catalysts: Influence of Calcination Temperature

Authors:

Anis Hamza Fakeeha, Yasir Arafat, Ahmed Aidid Ibrahim, Hamid Shaikh, Hanan Atia, Ahmed Elhag Abasaeed, Udo Armbruster, Ahmed Sadeq Al-Fatesh

Date Submitted: 2019-07-17

Keywords: ZrO₂, partial oxidation, methane, Syngas, bimetallic catalyst, Al₂O₃

Abstract:

In this study, Ni, Co and Ni/Co catalysts supported on binary oxide ZrO₂/Al₂O₃ were synthesized by sol-gel method and characterized by means of various analytical techniques such as XRD, BET, TPR, TPD, TGA, SEM, and TEM. This catalytic system was then tested for syngas respective H₂ production via partial oxidation of methane at 700 °C and 800 °C. The influence of calcination temperatures was studied and their impact on catalytic activity and stability was evaluated. It was observed that increasing the calcination temperature from 550 °C to 800 °C and addition of ZrO₂ to Al₂O₃ enhances Ni metal-support interaction. This increases the catalytic activity and sintering resistance. Furthermore, ZrO₂ provides higher oxygen storage capacity and stronger Lewis basicity which contributed to coke suppression, eventually leading to a more stable catalyst. It was also observed that, contrary to bimetallic catalysts, monometallic catalysts exhibit higher activity with higher calcination temperature. At the same time, Co and Ni/Co-based catalysts exhibit higher activity than Ni-based catalysts which was not expected. The Co-based catalyst calcined at 800 °C demonstrated excellent stability over 24 h on stream. In general, all catalysts demonstrated high CH₄ conversion and exceptionally high selectivity to H₂ (~98%) at 700 °C.

Record Type: Published Article

Submitted To: LAPSE (Living Archive for Process Systems Engineering)

Citation (overall record, always the latest version):

LAPSE:2019.0638

Citation (this specific file, latest version):

LAPSE:2019.0638-1

Citation (this specific file, this version):



LAPSE:2019.0638-1v1

DOI of Published Version: <https://doi.org/10.3390/pr7030141>

License: Creative Commons Attribution 4.0 International (CC BY 4.0)

Article

Highly Selective Syngas/H₂ Production via Partial Oxidation of CH₄ Using (Ni, Co and Ni–Co)/ZrO₂–Al₂O₃ Catalysts: Influence of Calcination Temperature

Anis Hamza Fakeeha ¹, Yasir Arafat ¹, Ahmed Aidid Ibrahim ¹, Hamid Shaikh ², Hanan Atia ^{3,*}, Ahmed Elhag Abasaed ¹ , Udo Armbruster ³ and Ahmed Sadeq Al-Fatesh ^{1,*} 

¹ Chemical Engineering Department, College of Engineering, King Saud University, P.O. Box 800, Riyadh 11421, Saudi Arabia; anishf@ksu.edu.sa (A.H.F.); engr.arafat111@yahoo.com (Y.A.); aidid@ksu.edu.sa (A.A.I.); abasaed@ksu.edu.sa (A.E.A.)

² Chemical Engineering Department, SABIC Polymer Research Center, King Saud University, P.O. Box 800, Riyadh 11421, Saudi Arabia; hamshaikh@ksu.edu.sa

³ Leibniz Institute for Catalysis, 18055 Rostock, Germany; udo.armbruster@catalysis.de

* Correspondence: hanan.atia@catalysis.de (H.A.); aalfatesh@ksu.edu.sa (A.S.A.-F.); Tel.: +49-3811281258 (H.A.); +966-14676859 (A.S.A.-F.)

Received: 7 February 2019; Accepted: 28 February 2019; Published: 6 March 2019



Abstract: In this study, Ni, Co and Ni–Co catalysts supported on binary oxide ZrO₂–Al₂O₃ were synthesized by sol-gel method and characterized by means of various analytical techniques such as XRD, BET, TPR, TPD, TGA, SEM, and TEM. This catalytic system was then tested for syngas respective H₂ production via partial oxidation of methane at 700 °C and 800 °C. The influence of calcination temperatures was studied and their impact on catalytic activity and stability was evaluated. It was observed that increasing the calcination temperature from 550 °C to 800 °C and addition of ZrO₂ to Al₂O₃ enhances Ni metal-support interaction. This increases the catalytic activity and sintering resistance. Furthermore, ZrO₂ provides higher oxygen storage capacity and stronger Lewis basicity which contributed to coke suppression, eventually leading to a more stable catalyst. It was also observed that, contrary to bimetallic catalysts, monometallic catalysts exhibit higher activity with higher calcination temperature. At the same time, Co and Ni–Co-based catalysts exhibit higher activity than Ni-based catalysts which was not expected. The Co-based catalyst calcined at 800 °C demonstrated excellent stability over 24 h on stream. In general, all catalysts demonstrated high CH₄ conversion and exceptionally high selectivity to H₂ (~98%) at 700 °C.

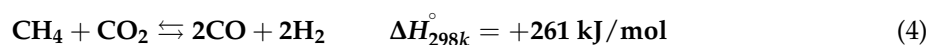
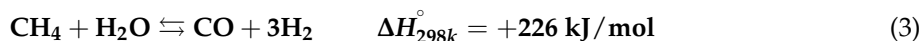
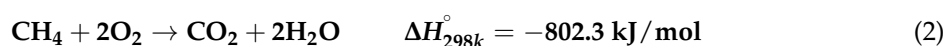
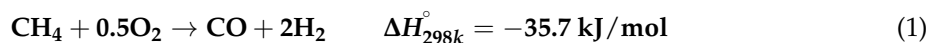
Keywords: Al₂O₃; bimetallic catalyst; syngas; methane; partial oxidation; ZrO₂

1. Introduction

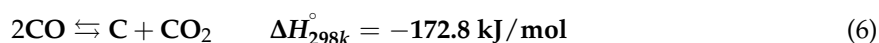
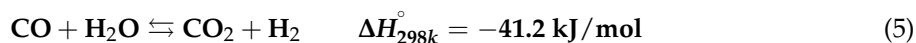
Methane (CH₄) is an important constituent of natural and biogas and plays an important role in C₁ chemistry. Its utilization is expected to increase in the future because of the weaker greenhouse gas effect (CO₂ release) compared to other fossil resources. However, it is well known that the direct conversion of methane yields less valuable petrochemical products and hence it is necessary to resort to an indirect process that initially involves the generation of synthesis gas (H₂ and CO) [1–4]. Synthesis gas is widely used in the production of hydrogen, synthetic fuels, alcohols and other chemicals. It can be produced by partial oxidation of hydrocarbons, particularly methane, via (i) steam reforming or (ii) dry reforming (DRM) or (iii) autothermal reforming. Specifically, the catalytic partial oxidation of methane has been recognized as a beneficial process from both technical and economic perspective; as it requires

less energy and capital cost due to low endothermic nature of the process [5]. In addition, the H₂/CO ratio of 2 is suitable for methanol synthesis and higher hydrocarbons through the Fischer-Tropsch process [6].

Various reaction mechanisms have been suggested for the partial oxidation of methane. The first is a direct route (Equation (1)) while the second mechanism comprises combustion and two reforming reactions. In the latter pathway, combustion of methane is accomplished (Equation (2)). Subsequently, steam and dry reforming of methane take place in the presence of the newly produced CO₂ and H₂O, respectively (Equations (3) and (4)) to render syngas.



Moreover, some side reactions, such as water gas shift reaction (Equation (5)) and Boudouard reaction (Equation (6)) can also occur along with main reactions.



The water gas shift and Boudouard reactions are exothermic in nature and take place at lower temperature. However, the respective reverse reactions occur upon increasing the reaction temperature.

Among the efficient catalysts for partial oxidation of methane (POM) are transition metals such as Ni, Pt, and Co supported on alumina, zirconia etc. However, these catalysts deactivate as a result of carbon formation [7,8]. It has been established that the activity of the Ni and/or Co catalysts not only relies on the structure and the nature of the active metals but selection of the support also plays a significant role. Al₂O₃ is extensively utilized as a support for reforming reactions. However, when Al₂O₃ is employed alone as a support for such type of catalysts, problems arise such as carbon deposition on active sites and development of inactive spinel phase (NiAl₂O₄) [9]. The modification of support, therefore, can be a promising route to enhance the catalytic performance. Among the prevalent materials, ZrO₂ has drawn considerable attention due to its excellent characteristics like acid-base properties, oxygen storage capacity and thermal stability [10]. It also inhibits the formation of spinels like NiAl₂O₄ by impeding the incorporation of active species into Al₂O₃ lattice [11,12]. Tetragonal zirconia is unstable at ambient temperature, but it can be stabilized by addition of Al₂O₃ to ZrO₂. Moreover, this binary system has a higher modulus of elasticity compared to neat ZrO₂ [11,13].

Several studies have been carried out on the formation of synthesis gas by using Ni and Co-based catalysts. Zagaynov et al. [14] examined Ni (Co)-Gd_{0.1}Ti_{0.1}Zr_{0.1}Ce_{0.7}O₂ mesoporous catalysts obtained by co-precipitation for partial oxidation and dry reforming of methane. Surprisingly, the results showed that Co and Ni-Co-containing catalysts were more active in partial oxidation of methane than the Ni sample, while Ni-catalysts were more active in dry reforming of methane. Calcination temperature, on the other hand, affects the active metal particle size and therefore alters the stability of the catalysts by changing the diffusion path. Moreover, the calcination temperature has a significant impact on the structural and catalytic properties of the catalysts, which interact strongly with the metal oxide support. Other researchers [15,16] also highlighted the effect of pretreatment of catalysts at calcination temperature. On the other hand, other studies have demonstrated comparable performance at high temperatures or by using precious metals. For instance, Dedov and co-workers utilized neodymium-calcium cobaltate-based catalysts for syngas production via partial oxidation of methane [17]. They reported to attain 85% methane conversion and selectivity of CO and H₂ close to 100% at very a high temperature (925 °C). Likewise, another study used Ni(Co)-Gd_{0.1}Ti_{0.1}Zr_{0.1}Ce_{0.7}O₂ catalyst and

obtained comparable H₂ selectivity at a higher temperature (900 °C) for the production of syngas via partial oxidation of methane [14]. The present work is driven by our previous work [18] where it has been shown that by using a single catalysis system of cobalt over CeO₂ and ZrO₂ supports; the hydrogen yield only up to 60% and 75 respectively was achieved for this system. Moreover, CeO₂ support yield low hydrogen and cobalt alone is considered less reforming catalysis. Therefore, in this work, the effect of binary metal system and support has been studied. It was observed that this system performs much better than single catalyst where hydrogen production was achieved up to 100%. Several studies have employed Co-based catalysts for reforming reactions [14,19,20]. For instance, Zagaynov et al. [14] examined (Ni, Co and Co-Ni)/-Gd0.1Ti0.1Zr0.1Ce0.7O₂ mesoporous catalysts obtained by co-precipitation for partial oxidation and dry reforming of methane. Interestingly, the results showed that the Co- and Ni-Co- containing catalysts exhibited excellent catalytic performance in partial oxidation of methane than the Ni sample, while the Ni-catalysts demonstrated tremendous catalytic performance in dry reforming of methane.

Accordingly, the significance of this research contribution was to obtain a high catalytic performance at relatively low temperature using mono and bimetallic Co and Ni supported on (ZrO₂ + Al₂O₃) which are capable of producing syngas via partial oxidation of methane. In addition, they must be stable to overcome the deactivation processes like carbon accumulation, metal agglomeration and thermal sintering. The study of catalyst design started with a systematic investigation of the desired reaction together with potential side reactions. The sol-gel method of preparation was proposed to generate strong metal-support interaction (MSI) and to produce smaller metal particles, which is expected to be active in the catalytic reaction.

2. Materials and Methods

2.1. Materials

The chemicals used in the present study were all of analytical grade and supplied by Aldrich, Gillingham, UK. They included cobalt acetate Co(ac)₂·4H₂O, nickel acetate Ni(ac)₂·4H₂O and zirconium(IV)-butoxide Zr(BuO)₄ (80 wt % solution in 1-butanol). Aluminum tri-sec-butylate Al(sec.-BuO)₃ was supplied by Merck, Southampton, UK.

2.2. Catalyst Preparation

The known sol-gel methods were adapted for the preparation of the catalysts. Precursors Co and Ni acetates were thoroughly dried to eliminate the moisture content. Then they were ground and sieved to obtain particle sizes <100 μm. The total metal loading is 5 wt % of Co and/or Ni in the monometallic catalyst, while for the bimetallic the total metal loading was 5 wt % with 1:1 mole ratio. The Zr to Al atoms is also 1:1 mole ratio. For the preparation of 16.33 g of ZrO₂-Al₂O₃ with an equimolar ratio of Zr to Al, 48 g of Zr-butylate (equivalent to 11.32 g of ZrO₂) and 25 g of Al-sec-butylate (equivalent to 5.01 g of Al₂O₃) were placed in a 250 mL three-necked round glass bottom flask. The mixture was heated with continuous stirring to 130 °C. A lot of 2.59 g of dried Co acetate was added and the mixture was again heated for about two hours at the same temperature.

After completion, the reaction mixture was transferred into 75 g of isopropanol. A homogeneous solution was obtained with slightly pink color when using Co while it was faint green in presence of Ni. To this solution, 27 mL of distilled water were added immediately and the mixture was then refluxed for another hour. After cooling to room temperature, the precipitate was separated from the liquid with a glass frit. The obtained solid was first dried at room temperature overnight and then divided into two parts. One part was calcined under air at 550 °C for 5 h with a heating rate of 2 K/min. The other part of the solid was calcined at 800 °C under similar conditions. For simplicity, the catalyst names refer to their pre-treatment calcination temperature.

2.3. Catalyst Testing

Catalyst activity measurements were carried out using a Process Integral Development Engineering and Technology (PID Eng & Tech) Microactivity Setup equipped with a tubular stainless steel fixed-bed reactor (9 mm I.D., Autoclave Engineers, Pennsylvania, USA). The effluent gases were analyzed by an on-line gas chromatograph (GC, ALPHA MOS instrument, Toulouse, France) with a thermal conductivity detector at an interval of 30 min. For separation of the products, two GC columns Molecular Sieve 5A and Porapak Q were employed in series/bypass connections. A catalyst load of 0.15 g was used for each run while the total gas flow was fixed at 15 mL/min. Prior to the reaction the catalyst was reduced by dosing H₂ at a flow rate of 40 mL/min. The temperature was kept at 800 or 700 °C and held for 1 h in order to reduce the metal oxide into the active metal. Afterwards, the reactor was purged with N₂ till the required reaction temperature was achieved. The feed is not introduced to the reactor unless H₂ is completely removed from the system. This is done using GC analysis via TCD detector. A propak Q and molecular sieve columns were used for separation. The volume ratio of feed gases (CH₄/O₂) was set to 2. In addition, the space velocity was held at 6000 mL/(h·g_{cat}), while the total feed rate was set to 15 mL/min. The reaction temperature was checked by placing a thermocouple in the middle of the catalyst bed and the bed height was 0.4 cm. The reforming activity of catalysts was studied at 700 and 800 °C at 1 bar.

The composition of effluent gases was calculated by the normalization method, and the equations for determination of conversion and selectivity are used as following:

$$\text{Conversion of CH}_4 : X_{\text{CH}_4} = \frac{\text{CH}_4 \text{ in} - \text{CH}_4 \text{ out}}{\text{CH}_4 \text{ in}} \times 100\% \quad (7)$$

$$\text{Selectivity of H}_2 : S_{\text{H}_2} = \frac{\text{moles of H}_2 \text{ produced}}{\text{Total moles of products (H}_2 + \text{H}_2\text{O)}} \times 100\% \quad (8)$$

$$\text{Selectivity of CO} : S_{\text{CO}} = \frac{\text{moles of CO produced}}{\text{Total moles of products (CO} + \text{CO}_2)} \times 100\% \quad (9)$$

2.4. Catalyst Characterization

Powder X-ray diffraction (XRD) analysis of fresh catalyst was conducted by employing a Rigaku (Miniflex) diffractometer with a Cu K α 1 radiation ($\lambda = 0.15406$ nm) operated at 40 mA and 40 kV. The 2θ range and scanning step for analysis were 10–80° and 0.02°, respectively.

The N₂ adsorption and desorption data at –196 °C was analyzed for determining the specific surface area (BET) of the fresh catalysts by using Micromeritics Tristar II 3020 surface area analyzer. In order to get rid of other adsorbed gases and moisture, all samples were degassed before analysis. For each analysis, a load of 0.2–0.3 g of catalyst was used. The pore size distribution of catalysts was calculated from the adsorption branch of N₂ isotherm by using the Barrett, Joyner & Halenda (BJH) method.

Temperature-programmed hydrogen reduction (H₂-TPR) and temperature-programmed carbon dioxide desorption (CO₂-TPD) measurements were performed on a chemisorption device (Micromeritics AutoChem II).

A known amount of catalyst was pre-treated with high purity argon (Ar) at 150 °C for about half an hour for TPR analysis. Then, the samples were heated in an automatic furnace to 1000 °C at a steady heating rate of 10 K/min under 40 mL/min of H₂/Ar mixture (volume ratio = 10/90) at atmospheric pressure. The H₂ signal was monitored by a thermal conduction detector (TCD).

For TPD experiments, first the adsorption of carbon dioxide onto the samples was carried out for half an hour at 50 °C under 10%CO₂/He gas at 30 mL/min. Then, the CO₂ desorption was done by increasing the temperature at a rate of 10 K/min to 800 °C.

The scanning electron microscopy (SEM) was employed in order to investigate the surface morphology of the catalysts. The SEM images of the spent catalyst samples were taken by using

JSM-7500F (JEOL Ltd., Tokyo, Japan) scanning electron microscope. The TEM study was carried out at 200 kV with an aberration-corrected JEM-ARM200F (JEOL, Corrector: CEOS). The microscope is fitted with a JED-2300 (JEOL) energy-dispersive X-ray-spectrometer for chemical analysis.

Temperature-programmed oxidation (TPO) experiments were conducted to determine the carbon accumulation on the spent catalyst after prolonged activity tests. The samples recovered from partial oxidation were dried at 150 °C for half an hour under helium at 30 mL/min and then cooled to ambient temperature. Afterwards, the temperature was raised with a ramp of 10 K/min to 800 °C under 10% O₂/He at 30 mL/min.

The quantitative analysis of coke deposition on the spent catalysts was carried out using thermo-gravimetric analyzer (Shimadzu, Kyoto, Japan). The spent catalysts weighing 10–15 mg were heated from ambient temperature to 1000 °C at a heating rate of 20 K/min, and the weight loss was recorded. For this purpose, catalyst samples recovered after 5 h on stream at 700 and 800 °C as well as Co-800 after long term test (24 h) at 800 °C were used. All analyses were carried out under air atmosphere.

3. Results and Discussion

3.1. X-ray Diffraction (XRD)

Typical XRD patterns in the range $2\theta = 10\text{--}80^\circ$ of fresh cobalt and/or nickel catalysts supported on the composite support (Al₂O₃ + ZrO₂) calcined at 550 and 800 °C are presented in Figure 1. In the case of samples calcined at 550 °C, broad reflections are observed. It is not possible to distinguish the species due to broadening and superimposing of reflections. Therefore, it implies that metal species are made of smaller crystallites and are well dispersed on the supports, which makes them amorphous and insensitive to X-ray radiations. This finding is consistent with the results obtained by BET and TPR which will be discussed later. Also, it is well known that the addition of zirconia to alumina leads to signal enlargement as a result of the formation of smaller particles [18,21]. Moreover, the decline in the intensity of the diffraction signals of catalysts Ni-550, Co-550 and Ni-Co-550 may also be caused by the distortion or defects in the Al-O bonds due to Zr presence in the support [22].

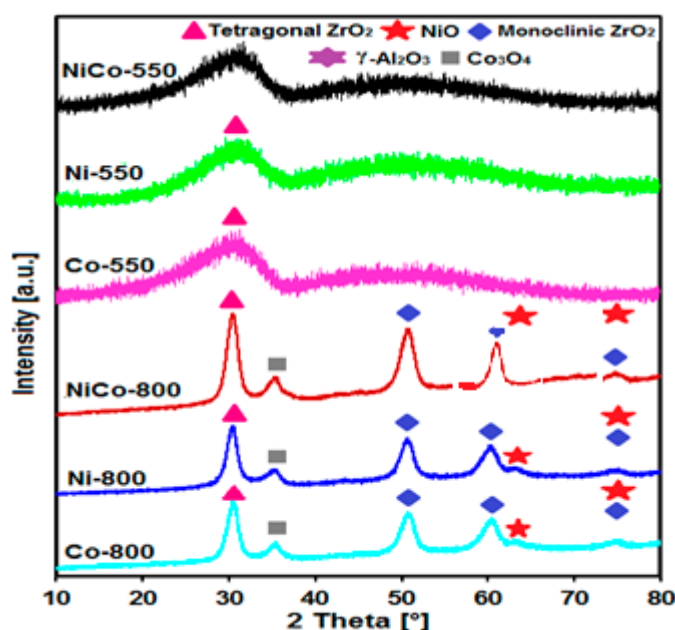


Figure 1. XRD patterns for fresh Ni and/or Co-based catalysts calcined at 550 and 800 °C.

With regard to the catalysts calcined at 800 °C, diffraction signals of sharp intensity observed; those represent more crystalline phases. Furthermore, the reflex intensity of the bimetallic catalyst is

higher than for the monometallic catalysts. For the Ni-800 catalyst, the reflections obtained at $2\theta = 63^\circ$, 75.3° and 79.4° are attributed to cubic NiO phase (JCPDS 01-73-1519). Actually, it is hard to identify the nickel oxide in the catalysts because its reflexes coincide with those of the tetragonal phase of zirconia [10]. The reflections observed at $2\theta = 50.2^\circ$, 59.9° , 62.8° and 75.2° are ascribed to monoclinic ZrO_2 (JCPDS: 00-007-0343). The signals found at $2\theta = 60.5^\circ$ may be assigned to $\gamma-Al_2O_3$ (JCPDS: 00-029-0063). Only in case of Ni-Co-800, extra peaks detected at $2\theta = 65.53^\circ$ and 66.4° correspond to the formation of $NiAl_2O_4$ spinel phase. It is noteworthy that for both mono- and bimetallic catalysts the increase of the calcination temperature increases the reflex intensity which may be attributed to the formation of larger crystal size.

3.2. Textural Properties

The surface texture was assessed by using the nitrogen adsorption–desorption isotherms. Figure 2 illustrates the adsorption isotherms of the fresh catalysts calcined at $550^\circ C$ and $800^\circ C$, while BET surface area, average pore diameter and pore volume are tabulated in Table 1. As per the IUPAC classification, catalysts demonstrate Type II isotherms. In Figure 2a it can be found that the BET surface area of Co-550 is highest and that of Ni-550 is lowest, while the surface area of Ni-Co-550 takes an intermediate value. On the other hand, the catalysts calcined at $800^\circ C$ (Figure 2b) exhibited a similar trend (Co > Ni-Co > Ni), however, the surface area of these catalysts was lower compared to those calcined at $550^\circ C$, which may be due to the sintering. In a previous study, we showed that the addition of ZrO_2 to Al_2O_3 increased the surface area. For instance, the surface area of pure supported Ni/ ZrO_2 and Ni/ Al_2O_3 catalysts were $3.1\text{ m}^2/\text{g}$ and $122.0\text{ m}^2/\text{g}$, respectively [23]. However, the surface area of binary supported Ni/ $Al_2O_3 + ZrO_2$ catalyst had risen to $212\text{ m}^2/\text{g}$.

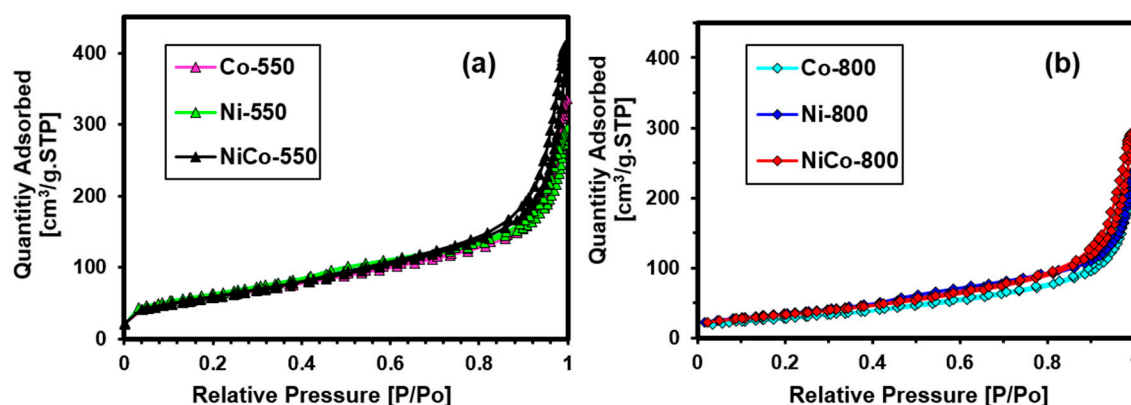


Figure 2. N_2 adsorption-desorption isotherms for fresh Ni and/or Co-based catalysts (a) calcined at $550^\circ C$ and (b) calcined at $800^\circ C$.

Table 1. BET surface area, pore volume (P.V.) and pore diameter (P.D.) of fresh Ni and/or Co-based catalysts calcined at $550^\circ C$ and $800^\circ C$.

Catalysts	BET Surface Area (m^2/g)	P.V. (cm^3/g)	P.D. (\AA)
Ni-550	212	0.51	100
Co-550	230	0.44	82
Ni-Co-550	216	0.61	114
Ni-800	105	0.37	134
Co-800	130	0.38	104
Ni-Co-800	123	0.47	142

3.3. Temperature-Programmed Reduction (H_2 -TPR)

In order to evaluate the reducibility of the species present in the catalyst, temperature-programmed reduction with hydrogen was employed. As shown in Figure 3a,b, Ni and/or Co catalysts calcined at

550 °C and 800 °C undergo a single-step reduction. NiO and CoO/Co₃O₄ are reducible species and can be categorized on the basis of their reduction temperature. As found in literature, bulk NiO is reduced between 300 and 400 °C [24,25]. In the case of the catalysts calcined at 550 °C (Figure 3a), a broad and pronounced reduction peak is observed for Ni-550 at 450–700 °C with a peak centered at 590 °C. This indicates that the Ni²⁺ species are difficult to reduce due to their interaction with the support (forming spinel) [26].

It is well known that the TPR profiles of cobalt catalysts demonstrate two distinct metal oxide species being reduced at specific temperature. First, region (<400 °C) is assigned to the reduction of Co₃O₄ to CoO. The second region (400–500 °C) corresponds to the reduction of CoO to metallic Co⁰ [27]. Therefore, the H₂ reduction peak with a maximum around 870 °C can be attributed to the reduction of Co²⁺ species with strong support interaction.

With regard to the bimetallic Ni–Co-550 catalyst, the combination of both Ni and Co enhances the reducibility of Co. The broadening of the reduction peak in the high-temperature zone may be attributed to the reduction of Ni–Co₂O₄ species forming Co–Ni alloy, having strong interaction with Al₂O₃ + ZrO₂ as proposed by our previous study [28]. It is noteworthy that the TPR peak area of Ni–Co-550 is higher than the monometallic one, suggesting that it possesses more reducible species. On the other hand, H₂-TPR conducted for the catalysts calcined at 800 °C (Figure 3b) followed the same trend. However, the position and the intensity of the peaks were different. In the case of Co-800, the single reduction peak may be designated to the overlapping of two-stage reduction of Co₃O₄ → CoO → Co metal [29,30]. The shift of reduction peaks suggests the existence of strong interaction between Co²⁺ and support due to calcination. The same shift was also observed for both Ni and bimetallic Ni–Co. Moreover, Co-800 was found to have the highest intensity and peak shift as it was found for the samples calcined at 550 °C.

In our system ZrO₂ obviously doesn't interact with Al₂O₃ strongly and the interaction between ZrO₂ and Ni is weak as was found by J. Asencios et al. [31] so Ni and/or Co is able to interact with Al₂O₃ to form Ni and/or CoAl₂O₄ and by this the Ni and/or Co are highly dispersed and as they are small crystals it is not possible to observe by XRD. The extent of this transformation increased with calcination temperature and is evidenced by the shift in reduction temperature for samples calcined at different temperatures. Also, G. P. Berrocal et al. [10] found that Ni strongly interacts with aluminum forming small NiAl₂O₄ particles that have the highest reduction temperature. At the same time, this sample showed the highest catalytic activity for the partial oxidation of methane. We observed similar dependency in our results.

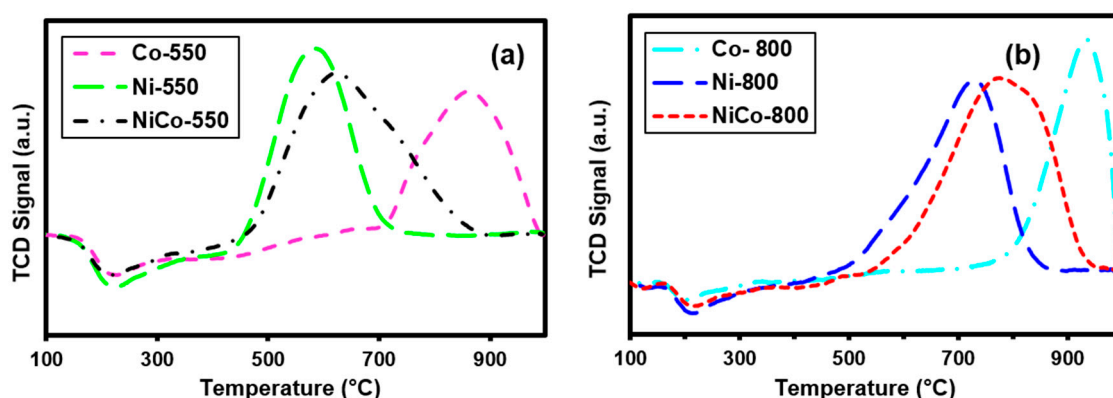


Figure 3. TPR profiles for fresh monometallic Ni or Co and bimetallic Ni–Co-based catalysts (a) calcined at 550 °C and (b) calcined at 800 °C.

3.4. Thermal Analysis for Carbon Deposition

TGA analysis was conducted to quantify the deposited carbon over the spent catalysts. In Figure 4a,b, the TGA profiles illustrate the weight loss (%) as a function of temperature for all

recovered catalysts from tests at 700 and 800 °C, respectively. In general, the amount of deposited carbon was relatively low for all the tested catalysts due to the presence of zirconia which is well known for high oxygen storage capacity and the presence of basic centers. The relative carbon deposition after reaction at 700 °C can be assigned in the following order: Ni-800 \approx Co-550 < Co-800 < Ni-550 < Ni-Co-800 < Ni-Co-550 (Figure 4b). For all catalysts, the burning of carbon starts at the same temperatures around 500 °C except for Ni-Co-550. From Figure 4 it is clear that Co-550 was the least prone to carbon deposition at both reaction temperatures 700 °C and 800 °C because cobalt is recognized as a strong oxidizing catalyst which can tackle the soot formation [32]. Interestingly, all catalysts calcined at 800 °C were found to have lower and similar amount of carbon deposits after reaction at 800 °C (encircled in Figure 4b), which can be associated to the strong interaction of metal species with composite support as it has been discussed in Section 3.3 [14]. Consequently, it can be deduced that higher calcination and reaction temperatures pose no adverse effect to our catalysts because they were less susceptible to carbon deposition. We assume that increasing the calcination temperature from 550 to 800 °C may form new surface sites due to the strong metal-support interaction. This might stabilize the high Ni and/or Co dispersion against metal agglomeration and deactivation. Apart from this, ZrO₂ might activate the oxidation of coke at high temperature and prevent the catalysts from coking. Also, Co-800 catalyst operated at 800 °C had excellent stability for 24 h on stream without deactivation (as it will be discussed latter). Henceforth, monometallic catalysts presented better performance with higher calcination temperature than bimetallic ones. In addition, the rate of coking over Ni-Co-800 was higher in comparison with mono-metallic catalysts which is consistent with the findings reported in the literature [33,34]. Moreover, this effect was more pronounced for the catalysts calcined at 550 °C (Figure 4a).

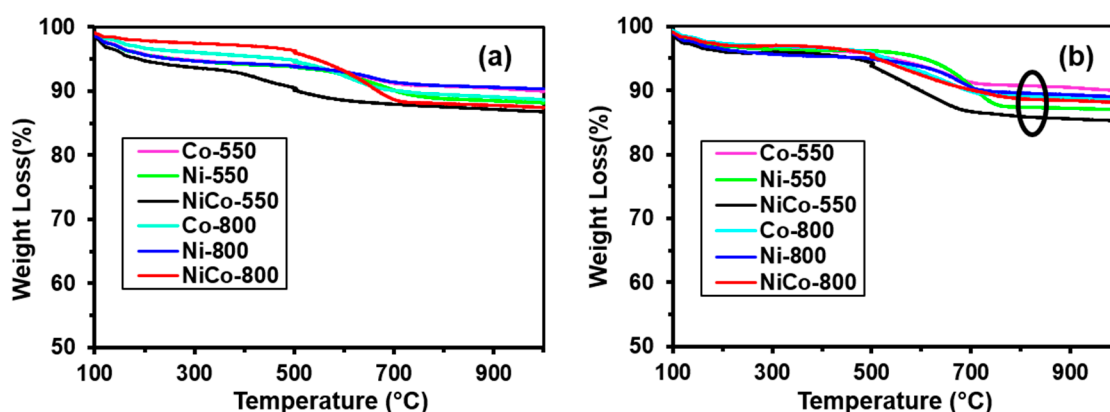


Figure 4. TGA profiles for spent Ni and/or Co-based catalysts calcined at 550 °C and at 800 °C after tests at (a) 700 °C and (b) 800 °C.

3.5. Temperature-Programmed Desorption of CO₂ (CO₂-TPD)

The basicity of the Ni and/or Co-containing catalysts was evaluated by adsorption and desorption of CO₂ on the basic sites at different temperatures. Figure 5 represents the CO₂-TPD profiles of the catalysts. The strength of basic sites can be classified by the temperature of the corresponding desorption peak of CO₂: weakly basic in the range of 50–200 °C, intermediate basic (200–400 °C), strongly basic (400–650 °C) and very strong basic sites (>650 °C) [35]. In fact, all these basic sites are evident from CO₂-TPD profiles, which reveal the strong basic character of the catalysts (Figure 5). Al₂O₃ as an acidic support favors coke formation. Therefore, ZrO₂ addition has rendered the catalysts basic character, which in turn escalated CO₂ adsorption contributing to higher activity and coke removal.

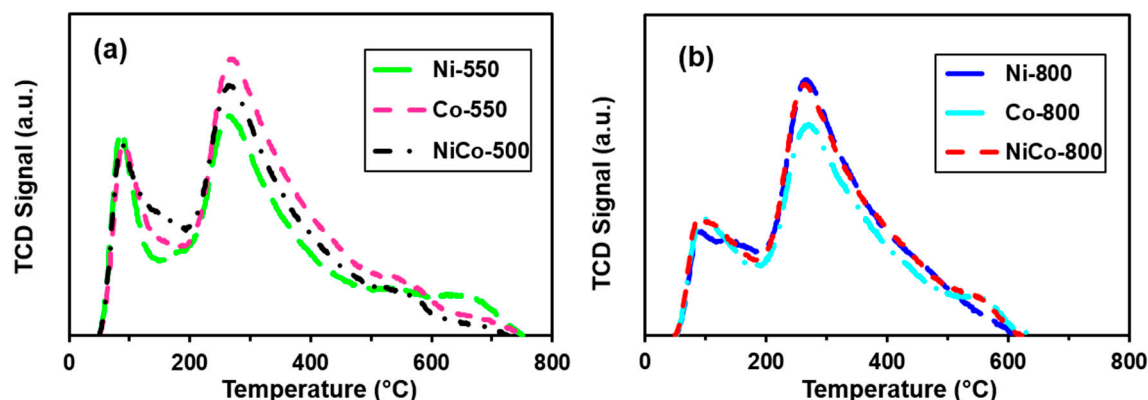


Figure 5. CO₂-TPD profiles for fresh Ni and/or Co-based catalysts after calcination at (a) 550 °C and (b) 800 °C.

3.6. Scanning Electron Microscopy (SEM) and Transmission Electron Microscopy (TEM)

Figure 6 displays SEM images of fresh and spent catalysts obtained after five hours on stream at 700 °C and corresponding samples calcined at 550 °C. The fresh catalyst surface shows a fairly good distribution of the particles while the spent catalyst shows agglomeration of the particles and therefore the surface area and Ni dispersion decrease. The catalytic activity is strongly affected by carbon deposition over the catalysts' surfaces, finally deactivating the catalyst.

TEM of Co/(Al₂O₃-ZrO₂) catalyst calcined at 800 °C used in the long term POM test at 800 °C reveals presence of filamentous coke and the size of carbon nanotubes (CNTs) is determined by the size of starting metallic species. These CNTs gradually grow and metallic Co species settled on the tip of the CNTs. As the metallic species are still exposed to the reacting gases, these CNTs do not show an adverse effect on activity because metallic species are still accessible [28].

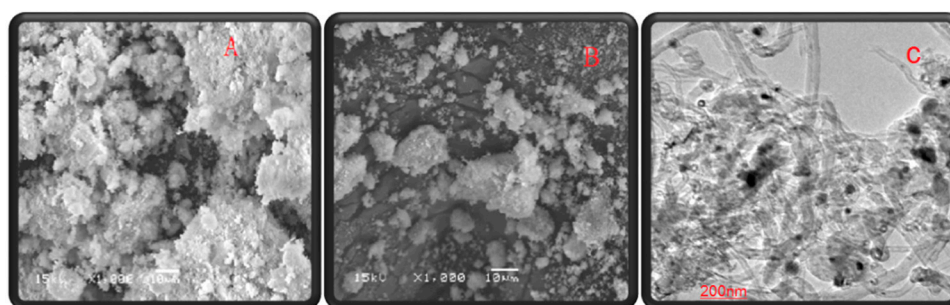


Figure 6. SEM images of Co-Ni/(Al₂O₃-ZrO₂) catalyst. (A) fresh catalyst, (B) spent catalyst calcined at 800 °C and operated at 700 °C reaction for 5 h and (C) TEM of Co/(Al₂O₃-ZrO₂) catalyst calcined at 800 °C after recovery from long term POM test (24 h) at 800 °C.

3.7. Catalytic Activity

The product H₂/CO ratio for all catalysts is slightly higher than the stoichiometric value of 2 (Figure 7), owing to the incomplete conversion of CO₂ (from combustion, Equation (1)) to CO. Also, a part of CO was consumed by the side reactions such as water-gas shift (Equation (5)) and Boudouard reactions (Equation (6)). Consequently, both of these effects lower the CO selectivity (Figure 8b) with time on stream and thus increase the H₂/CO ratio at 700 °C. Moreover, Co-800 gave the lowest CO₂ selectivity (15.2%) and the highest CO selectivity (85%), eventually attained H₂/CO ratio approaching the stoichiometric value of 2. It is worth to mention that the selectivity for hydrogen reached 98.6% for all catalysts at 700 °C.

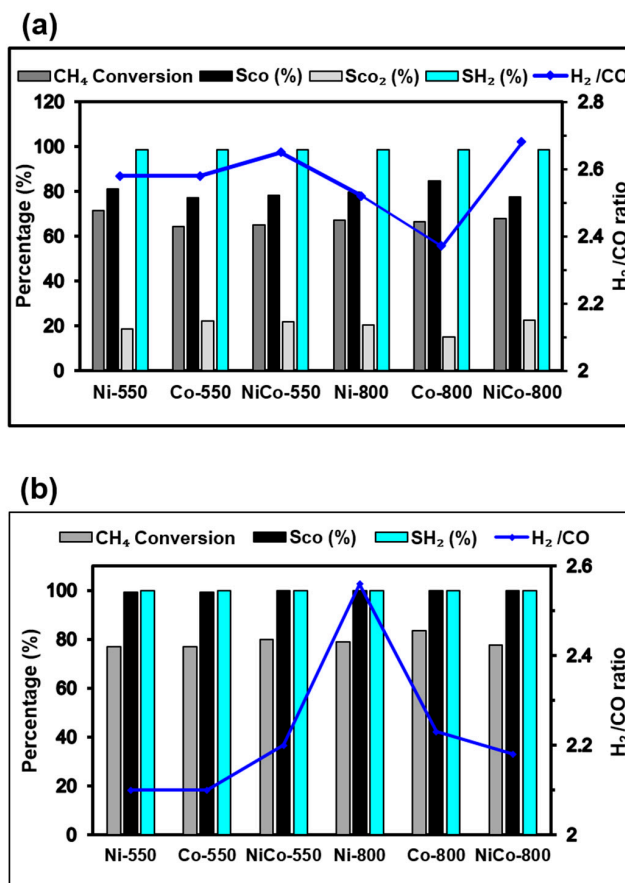


Figure 7. Conversion, selectivity and H₂/CO ratio obtained for Ni and/or Co-based catalysts operated at (a) 700 °C and (b) 800 °C.

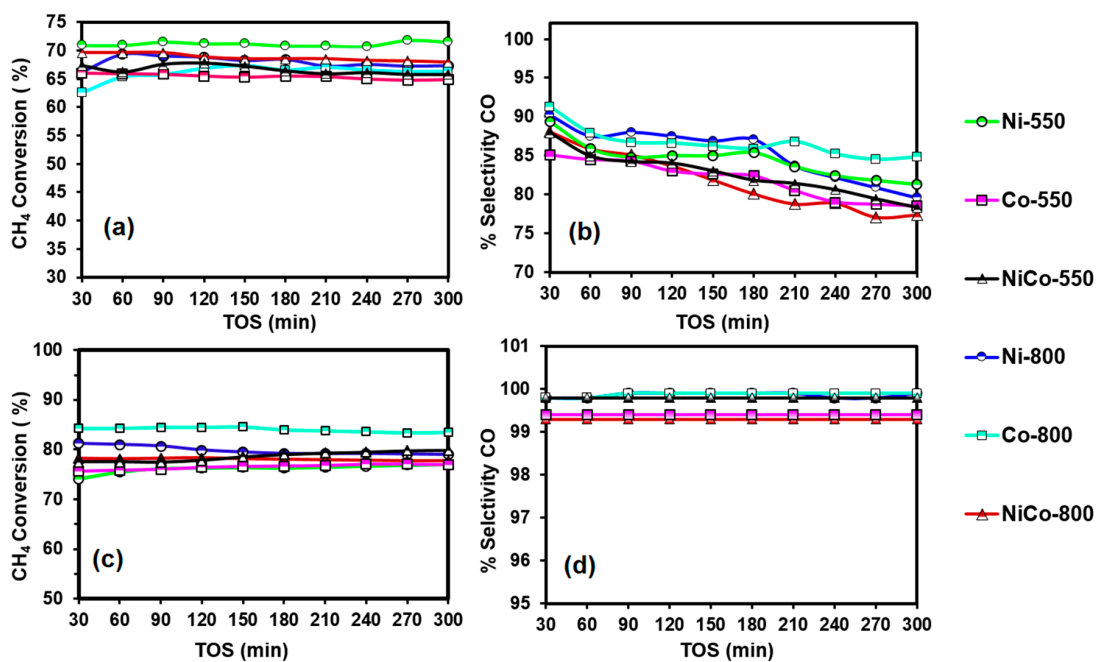


Figure 8. (a) CH₄ conversion and (b) CO selectivity with time on stream in POM over Ni and/or Co-based catalysts at 700 °C; (c) CH₄ conversion and (d) CO selectivity with time on stream in POM over Ni and/or Co-based catalysts at 800 °C.

The performance of the Ni/ZrO₂-Al₂O₃, Co/ZrO₂-Al₂O₃ and Co-Ni/ZrO₂-Al₂O₃ catalysts calcined at 550 °C and 800 °C was tested at 700 °C and 800 °C (Figure 8). Generally, the activity of catalysts progressively increases with rise in the reaction temperature. The oxygen conversion was unaltered (nearly 98%) for all catalysts irrespective of calcination temperatures. At 700 °C (Figure 8a) maximum conversion of 71.5% was achieved with the Ni-550 catalyst. This might be attributed to its high surface area compared to the other catalysts (Figure 2). It may also be due to minimum carbon deposition formed on this catalyst as shown in Figure 4. On the other hand, the activity of the bimetallic catalyst suffered from the formation of carbon deposits (Figure 4a,b). The lower activity of Ni-Co-800 catalyst may also be due to the formation of spinel phase as it was discussed with the help of TPR (Figure 1). These species are irreducible and do not contribute to methane conversion [36]. Since Al³⁺ and Ni²⁺ are located in the same lattice, the generation of the solid solution of NiAl₂O₄ spinel is conducive under higher calcination temperatures what about ZrO₂ [11]. Moreover, the highest selectivity for H₂ of 99% is achieved with all the catalysts when operated at 700 °C. As steam reforming (Equation (3)) is thermodynamically feasible at this temperature and water is available, it contributes to the rise in selectivity to H₂.

Generally, when the partial oxidation was carried out at 800 °C, both CH₄ conversion and CO selectivity were remarkably increased (Figure 7b). Moreover, methane conversion for all catalysts was found to be in the order: Co-800 > Ni-Co-550 > Ni-800 > Ni-Co-800 ≈ Ni-550 = Co-550. The selectivities to CO and H₂ achieved with all the catalysts exceeded 99% at 800 °C. In addition, the amount of CO₂ was minimum (<1%) in the product stream which implies that CO₂ has been converted into CO. All the catalysts maintained their activity throughout the test duration, which can be associated to the higher calcination temperature and the presence of ZrO₂. An intimate contact with metal species is developed by the presence of ZrO₂ due to strong electrostatic attraction between them. This fact is also evident from the TPR profiles. Furthermore, the strong metal-support interaction in these catalysts is responsible for the low carbon deposition.

Interestingly, when comparing to other catalysts, it was found that the monometallic Co-800 was the most active (84% CH₄ conversion) and stable catalyst (Figure 8c). In the presence of ZrO₂, the interaction between Al₂O₃ and Ni and/or Co increases. Ni and/or Co deposit on the support and develop an intimate contact which results in the modification of Al₂O₃ support [6]. The TPR of the monometallic sample Co-800 showed the highest reduction temperature due to the formation of stable spinel structures with the support. These interactions probably assist in dispersing the metals and coke formation resistance. The slight decline in the methane conversion of Ni-800 may be ascribed to blocking of active sites by carbon deposits (Figure 4) and relatively lower basicity (Figure 5). Similarly, at 800 °C the selectivity to CO remained constant throughout the stability test for all tested catalysts (Figure 8d). Consequently, the rise in the CO selectivity at 800 °C shifted the H₂/CO ratio to a value closer to 2. It is worth to mention that the reaction temperature of 800 °C is most favorable for reduction of the tested metal oxides as can be seen in TPR profiles (Figure 3). A similar study was conducted using the same catalyst Ni/(ZrO₂ + Al₂O₃) but employing a higher metal loading (8%) and a calcination temperature of 550 °C. The catalyst achieved almost comparable methane conversions, but higher amount of carbon deposits and significantly lower selectivity to CO and H₂ [10]. The comparison of this result with the present study suggests that calcination temperature has a significant influence on the catalytic performance.

The higher activity of bimetallic catalyst Ni-Co-550 can be attributed to the synergistic effect between Ni and Co which is in agreement with several findings [14]. This effect induces higher BET surface area, smaller crystallite size (XRD) and improved degree of reducibility (TPR). Co- and Ni-Co-based catalysts presented higher catalytic activity than Ni-based catalysts. This finding is consistent with recent studies conducted by Zagaynov and co-workers using (Ni, Co and Co-Ni)/-Gd_{0.1}Ti_{0.1}Zr_{0.1}Ce_{0.7}O₂ catalysts [14]. However, the decline in activity of Ni-Co-800 calcined at 800 °C may be ascribed to the formation of spinel phases as described above. On the basis of catalytic activity, Co-800 is the most promising catalyst giving higher conversion and excellent selectivity

to CO (85%) as well as H₂ (98.6%) even at 700 °C, and this selectivity can reach 100% at 800 °C reaction temperature. Therefore, it is evident that the monometallic catalysts gave better performance with higher calcination temperature while bimetallic catalysts exhibit higher activity with lower calcination temperature.

3.8. Long-Term Stability Test

Generally, catalyst stability in POM is greatly influenced by deactivation resulting from sintering, metal agglomeration, carbon deposition, and the disappearance of active sites due to oxidation at reaction conditions. Usually, these deactivation effects occur simultaneously, but sometimes one of them predominates. Among the catalysts used in this study, Co-800 showed best results and so it was selected for a prolonged activity test at 800 °C for 24 h (Figure 9). It is worth to mention that the catalyst maintained stable activity throughout the complete run.

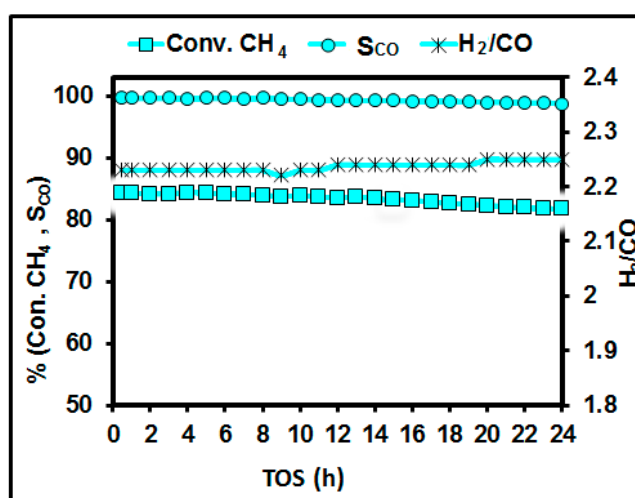


Figure 9. CH₄ conversion, CO selectivity and H₂/CO ratio over Co-800 (5%Co/Al₂O₃-ZrO₂) catalyst calcined at 800 °C over 24 h on stream in POM at 800 °C.

The stable activity may be attributed to the presence of ZrO₂ that leads to coke suppression as revealed by TGA and TPO (Figure 10). The presence of ZrO₂ imparts two advantages to the catalysts: (i) It renders basic character (Figure 5) to the catalysts which in turn makes it capable of activating CO₂ (CO₂ → CO + O*) because it enhances the dissociative chemisorption of CO₂ in metal/ZrO₂ interface; (ii) it suppresses the carbon deposition as an outcome of its higher oxygen storage capacity which provides more active oxygen species by redox activity (C* + O* → CO). This is the reason why the catalysts showed very low coking, making them long-term stable. Similar studies were conducted using Pt/Al₂O₃-ZrO₂ and Ni/Al₂O₃-ZrO₂ catalysts; higher activity and stability to syngas were reported [37,38]. This behavior is due to the rise in capacity of dissociative chemisorption of CO₂ over Pt-ZrO₂ and Ni-ZrO₂. Therefore, based on the stability analysis, it can be concluded that the catalyst operated at 800 °C was more stable than the one tested at 700 °C (Figure 8a–d).

3.9. Post (Long Term Test) Characterizations

Temperature-programmed oxidation (TPO) was conducted to characterize the nature of coke deposit over Co-800 catalyst after the long-term POM test (Figure 10a). Zhang investigated the TPO profiles for reforming reaction and assigned three peaks as C α (150–220 °C), C β (530–600 °C) and C γ (~650 °C) whereas the peak above 700 °C might indicate the oxidation of graphitic/inactive carbon [39]. We applied this model to our catalysts. As per TPO profile, the intensity maxima of C α was found at 293 °C corresponding to the most active carbon which is responsible for the transformation into synthesis gas. The maximum at 593 °C represents C β which may be attributed

to intermediate amorphous carbon and could be transformed into CO at high temperature. Finally, the peak at 665 °C possessing the lowest intensity may be ascribed to C_γ , an inert carbon intermediate which is transformed into filamentous or graphitic features. The intensity of the signal for the most active carbon (C_α) is higher which implies that these species are predominant. These findings are in agreement with TEM images (Figure 6c). When TGA (Figure 10b) was performed after the test over 24 h with Co-800 catalyst at 800 °C, it was found that there was insignificant (<1%) rise in the coke amount on the catalyst surface. The low amount of carbon may be attributed to the much amount of active and amorphous carbon type which is also registered by TPO.

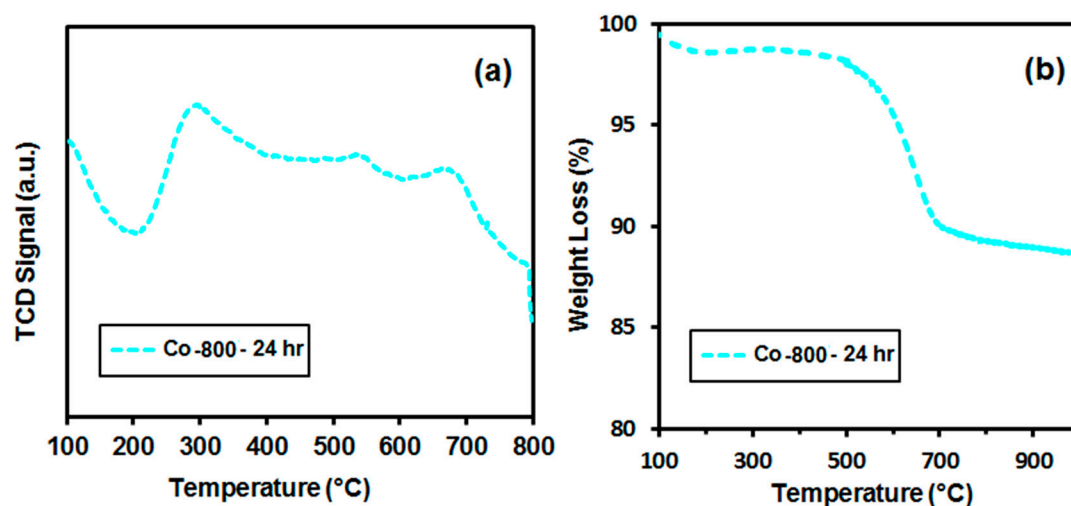


Figure 10. (a) Temperature-programmed oxidation and (b) TGA for Co-800 (5%Co/Al₂O₃—rO₂) catalyst calcined at 800 °C after the long-term POM test at 800 °C.

4. Conclusions

The obtained results show that the ZrO₂–Al₂O₃-supported Ni and/or Co catalysts for syngas production via partial oxidation exhibit a high surface area. Co/Al₂O₃–ZrO₂ catalysts demonstrated superior catalytic performance, giving high methane conversion and selectivity to CO and H₂ at 700 °C and reached up to 100% selectivity to H₂ and 84% methane conversion at 800 °C. Increasing the calcination temperature from 550 °C to 800 °C resulted in strong metal-support interaction which endowed resistance against sintering. The presence of ZrO₂ in the binary oxide enhanced the surface area and number of basic sites in the catalysts. Several factors can assist to obtain stable and active catalysts as the presence of basic sites by addition of ZrO₂-facilitated CO₂ dissociation, generation of oxygen intermediates, and removal of deposited carbon over the catalyst surface. Furthermore, the effect of calcination at a higher temperature of 800 °C stabilizes high dispersion of Ni and/or Co on the support, thereby avoiding metal agglomeration which in turn improved coke resistance. Eventually, monometallic Co-based catalyst calcined at 800 °C was found to have the highest activity but not Ni-based catalyst, which is unexpected. On the other hand, bimetallic Ni–Co-550 showed highest activity at low calcination temperature. Finally, increasing the calcination and reaction temperatures led to higher activity but posed no adverse effects on stability. It is worth mentioning that Co-800 catalyst used at 800 °C was found to have excellent stability over 24 h on stream. Recently, Dedov and co-workers utilized neodymium-calcium cobaltate-based catalysts for syngas production via partial oxidation of methane by using a fixed-bed flow reactor [17]. They reportedly attained 85% methane conversion and selectivity of CO and H₂ close to 100% at very high temperature (925 °C). Another study used Ni(Co)–Gd_{0.1}Ti_{0.1}Zr_{0.1}Ce_{0.7}O₂ catalyst at 900 °C for the production of syngas via partial oxidation of methane [14]. They obtained 80–90% methane conversion, 85–95% selectivity for CO and 79% selectivity for H₂. Methane conversion was somewhat higher but the selectivity to CO and H₂

was still lower even at a higher temperature. Based on the activity of catalysts reported in previous studies, our catalysts showed higher activity and selectivity at lower temperature.

Author Contributions: A.S.A.-F., A.H.F. and Y.A. carried out all experiments and characterization tests as well as shared in the analysis of the data and writing of the manuscript. U.A., H.A. and A.E.A. wrote the paper and shared data analysis. H.S. and A.A.I. contributed in writing the paper and edited it.

Funding: The research is funded by Deanship of Scientific Research at King Saud University project No. RGP-119.

Acknowledgments: The authors would like to extend their sincere appreciation to the Deanship of Scientific Research at King Saud University for funding this research group No. RGP-119.

Conflicts of Interest: The authors declare no conflict of interest.

References

1. Liu, Y.; Wang, T.; Li, Q.; Wang, D. A Study of Acetylene Production by Methane Flaming in a Partial Oxidation Reactor. *Chin. J. Chem. Eng.* **2011**, *19*, 424–433. [[CrossRef](#)]
2. Chibane, L.; Djellouli, B. Role of Periodic Input Composition and Sweeping Gas for Improvement of Hydrogen Production in a Palladium Membrane Reactor by Partial Oxidation of Methane. *Chin. J. Chem. Eng.* **2012**, *20*, 577–588. [[CrossRef](#)]
3. Dong, X.; Zhang, H.; Lin, W. Preparation and Characterization of a Perovskite-type Mixed Conducting $\text{SrFe}_{0.6}\text{Cu}_{0.3}\text{Ti}_{0.1}\text{O}_{3-\delta}$ Membrane for Partial Oxidation of Methane to Syngas. *Chin. J. Chem. Eng.* **2008**, *16*, 411–415. [[CrossRef](#)]
4. Fakeeha, A.H.; Al-Fatesh, A.S.; Chowdhury, B.; Ibrahim, A.A.; Khan, W.U.; Hassan, S.; Sasudeen, K.; Abasaheed, A.E. Bi-metallic catalysts of mesoporous Al_2O_3 supported on Fe, Ni and Mn for methane decomposition: Effect of activation temperature. *Chin. J. Chem. Eng.* **2018**, *26*, 1904–1911. [[CrossRef](#)]
5. Jun, J.H.; Lee, S.J.; Lee, S.H.; Lee, T.J.; Kong, S.J.; Lim, T.H.; Nam, S.W.; Hong, S.A.; Yoon, K.J. Characterization of a nickel-strontium phosphate catalyst for partial oxidation of methane. *Korean J. Chem. Eng.* **2003**, *20*, 829–834. [[CrossRef](#)]
6. Nichio, N.; Casella, M.; Ferretti, O.; Gonzalez, M.; Nicot, C.; Moraweck, B.; Frety, R. Partial oxidation of methane to synthesis gas. Behaviour of different Ni supported catalysts. *Catal. Lett.* **1996**, *42*, 65–72. [[CrossRef](#)]
7. Singha, R.K.; Shukla, A.; Yadav, A.; Konathala, L.S.; Bal, R. Effect of metal-support interaction on activity and stability of Ni-CeO₂ catalyst for partial oxidation of methane. *Appl. Catal. Environ.* **2017**, *202*, 473–488. [[CrossRef](#)]
8. Ding, C.; Ai, G.; Zhang, K.; Yuan, Q.; Han, Y.; Ma, X.; Wang, J.; Liu, S. Coking resistant Ni/ZrO₂@SiO₂ catalyst for the partial oxidation of methane to synthesis gas. *Int. J. Hydrog. Energy* **2015**, *40*, 6835–6843. [[CrossRef](#)]
9. Wu, P.; Li, X.; Ji, S.; Lang, B.; Habimana, F.; Li, C. Steam reforming of methane to hydrogen over Ni-based metal monolith catalysts. *Catal. Today* **2009**, *146*, 82–86. [[CrossRef](#)]
10. Berrocal, G.P.; Da Silva, A.L.; Assaf, J.M.; Albornoz, A.; do Carmo Rangel, M. Novel supports for nickel-based catalysts for the partial oxidation of methane. *Catal. Today* **2010**, *149*, 240–247. [[CrossRef](#)]
11. Sharifi, M.; Haghighi, M.; Rahmani, F.; Karimipour, S. Syngas production via dry reforming of CH₄ over Co- and Cu-Promoted Ni/Al₂O₃-ZrO₂ nanocatalysts synthesized via sequential impregnation and sol-gel methods. *J. Nat. Gas Sci. Eng.* **2014**, *21*, 993–1004. [[CrossRef](#)]
12. Therdthianwong, S.; Siangchin, C.; Therdthianwong, A. Improvement of coke resistance of Ni/Al₂O₃ catalyst in CH₄/CO₂ reforming by ZrO₂ addition. *Fuel Process. Technol.* **2008**, *89*, 160–168. [[CrossRef](#)]
13. Song, J.H.; Han, S.J.; Yoo, J.; Park, S.; Kim, D.H.; Song, I.K. Hydrogen production by steam reforming of ethanol over Ni-X/Al₂O₃-ZrO₂ (X = Mg, Ca, Sr, and Ba) xerogel catalysts: Effect of alkaline earth metal addition. *J. Mol. Catal. Chem.* **2016**, *415*, 151–159. [[CrossRef](#)]
14. Zagaynov, I.; Loktev, A.; Arashanova, A.; Ivanov, V.; Dedov, A.; Moiseev, I. Ni (Co)-Gd_{0.1}Ti_{0.1}Zr_{0.1}Ce_{0.7}O₂ mesoporous materials in partial oxidation and dry reforming of methane into synthesis gas. *Chem. Eng. J.* **2016**, *290*, 193–200. [[CrossRef](#)]

15. Weng, W.Z.; Pei, X.Q.; Li, J.M.; Luo, C.R.; Liu, Y.; Lin, H.Q.; Huang, C.J.; Wan, H.L. Effects of calcination temperatures on the catalytic performance of Rh/Al₂O₃ for methane partial oxidation to synthesis gas. *Catal. Today* **2006**, *117*, 53–61. [[CrossRef](#)]
16. Sokolov, S.; Kondratenko, E.V.; Pohl, M.-M.; Rodemerck, U. Effect of calcination conditions on time on-stream performance of Ni/La₂O₃-ZrO₂ in low-temperature dry reforming of methane. *Int. J. Hydrog. Energy* **2013**, *38*, 16121–16132. [[CrossRef](#)]
17. Dedov, A.G.; Loktev, A.S.; Komissarenko, D.A.; Parkhomenko, K.V.; Roger, A.C.; Shlyakhtin, O.A.; Mazo, G.N.; Moiseev, I.I. High-selectivity partial oxidation of methane into synthesis gas: The role of the redox transformations of rare earth-alkali earth cobaltate-based catalyst components. *Fuel Process. Technol.* **2016**, *148*, 128–137. [[CrossRef](#)]
18. Abasaeed, A.E.; Al-Fatesh, A.S.; Naeem, M.A.; Ibrahim, A.A.; Fakeeha, A.H. Catalytic performance of CeO₂ and ZrO₂ supported Co catalysts for hydrogen production via dry reforming of methane. *Int. J. Hydrog. Energy* **2015**, *40*, 6818–6826. [[CrossRef](#)]
19. Enger, B.C.; Lødeng, R.; Anders Holmen, A. Modified cobalt catalysts in the partial oxidation of methane at moderate temperatures. *J. Catal.* **2009**, *262*, 188–198. [[CrossRef](#)]
20. Lødeng, R.; Bjørgum, E.; Christian, B.; Enger Eilertsen, J.L.; Anders Holmen, A.; Krogh, B.; Rønnekleiv, M.; Erling Rytter, E. Catalytic partial oxidation of CH₄ to H₂ over cobalt catalysts at moderate temperatures. *Appl. Catal.* **2007**, *333*, 11–23. [[CrossRef](#)]
21. Silver, R.G.; Hou, C.J.; Ekerdt, J.G. The role of lattice anion vacancies in the activation of CO and as the catalytic site for methanol synthesis over zirconium dioxide and yttria-doped zirconium dioxide. *J. Catal.* **1989**, *118*, 400–416. [[CrossRef](#)]
22. Li, G.; Li, W.; Zhang, M.; Tao, K. Morphology and hydrodesulfurization activity of CoMo sulfide supported on amorphous ZrO₂ nanoparticles combined with Al₂O₃. *Appl. Catal.* **2004**, *273*, 233–238. [[CrossRef](#)]
23. Naeem, M.A.; Al-Fatesh, A.S.; Abasaeed, A.E.; Fakeeha, A.H. Activities of Ni-based nano catalysts for CO₂-CH₄ reforming prepared by polyol process. *Fuel Process. Technol.* **2014**, *122*, 141–152. [[CrossRef](#)]
24. Klein, J.C.; Hercules, D.M. Surface characterization of model Urushibara catalysts. *J. Catal.* **1983**, *82*, 424–441. [[CrossRef](#)]
25. Mile, B.; Stirling, D.; Zammitt, M.A.; Lowell, A.; Webb, M. The location of nickel oxide and nickel in silica-supported catalysts: Two forms of “NiO” and the assignment of temperature-programmed reduction profiles. *J. Catal.* **1998**, *114*, 217–229. [[CrossRef](#)]
26. Kim, P.; Kim, Y.; Kim, H.; Song, I.K.; Yi, J. Synthesis and characterization of mesoporous alumina with nickel incorporated for use in the partial oxidation of methane into synthesis gas. *Appl. Catal.* **2004**, *272*, 157–166. [[CrossRef](#)]
27. Arone, S.; Bagnasco, G.; Busca, G.; Lisi, L.; Russo, G.; Turco, M. Catalytic combustion of methane over transition metal oxides. *Stud. Surf. Sci. Catal.* **1998**, *119*, 65–70.
28. Al-Fatesh, A.S.; Arafat, Y.; Ibrahim, A.A.; Atia, H.; Fakeeha, A.H.; Armbruster, U.; Abasaeed, A.E.; Frusteri, F. Evaluation of Co-Ni/Sc-SBA-15 as a novel coke resistant catalyst for syngas production via CO₂ reforming of methane. *Appl. Catal.* **2018**, *567*, 102–111. [[CrossRef](#)]
29. Jongsomjit, B.; Panpranot, J.; Goodwin, J.G. Effect of zirconia-modified alumina on the properties of Co/ γ -Al₂O₃ catalysts. *J. Catal.* **2003**, *215*, 66–77. [[CrossRef](#)]
30. Jongsomjit, B.; Sakdamnusun, C.; Goodwin, J.G.; Praserthdam, P. Co-support compound formation in titania-supported cobalt catalyst. *Catal. Lett.* **2004**, *94*, 209–215. [[CrossRef](#)]
31. Asencios, Y.J.O.; Nascente, P.A.P.; Assaf, E.M. Partial oxidation of methane on NiO-MgO-ZrO₂ catalysts. *Fuel* **2012**, *97*, 630–637. [[CrossRef](#)]
32. Harrison, P.G.; Ball, I.K.; Daniell, W.; Lukinskas, P.; Céspedes, M.A.; Miró, E.E.; Ulla, M.A.A. Cobalt catalysts for the oxidation of diesel soot particulate. *Chem. Eng. J.* **2003**, *95*, 47–55. [[CrossRef](#)]
33. Rui, Z.; Feng, D.; Chen, H.; Ji, H. Anodic TiO₂ nanotube array supported nickel-noble metal bimetallic catalysts for activation of CH₄ and CO₂ to syngas. *Int. J. Hydrog. Energy* **2014**, *39*, 16252–16261. [[CrossRef](#)]
34. Djinić, P.; Črnivec, I.G.O.; Erjavec, B.; Pintar, A. Influence of active metal loading and oxygen mobility on coke-free dry reforming of Ni-Co bimetallic catalysts. *Appl. Catal.* **2012**, *125*, 259–270. [[CrossRef](#)]
35. Al-Fatesh, A.S.; Arafat, Y.; Atia, H.; Ibrahim, A.A.; Manh Ha, Q.L.; Schneider, M.; Pohl, M.M.; Fakeeha, A.H. CO₂-reforming of methane to produce syngas over Co-Ni/SBA-15 catalyst: Effect of support modifiers (Mg, La and Sc) on catalytic stability. *J. CO₂ Util.* **2017**, *21*, 395–404. [[CrossRef](#)]

36. Lu, Y.; Liu, Y.; Shen, S. Design of stable Ni catalysts for partial oxidation of methane to synthesis gas. *J. Catal.* **1998**, *177*, 386–388. [[CrossRef](#)]
37. Pompeo, F.; Nichio, N.N.; Ferretti, O.A.; Resasco, D. Study of Ni catalysts on different supports to obtain synthesis gas. *Int. J. Hydrog Energy* **2005**, *30*, 1399–1405. [[CrossRef](#)]
38. Souza, M.; Aranda, D.; Scmal, M. Reforming of Methane with Carbon Dioxide over Pt/ZrO₂/Al₂O₃ Catalysts. *J. Catal.* **2001**, *204*, 498–511. [[CrossRef](#)]
39. Zhang, Z.; Verykios, X. Carbon dioxide reforming of methane to synthesis gas over supported Ni catalysts. *Catal. Today* **1994**, *21*, 589–595. [[CrossRef](#)]



© 2019 by the authors. Licensee MDPI, Basel, Switzerland. This article is an open access article distributed under the terms and conditions of the Creative Commons Attribution (CC BY) license (<http://creativecommons.org/licenses/by/4.0/>).